AD-A089 265 ROYAL SIGNALS AND RADAR ESTABLISHMENT MALVERN (ENGLAND) F/G 14/2
DEVELOPMENTS IN UNITED KINGDOM WAVEGUIDE POWER STANDARDS.(U)
APR 80 P J SKILTON
UNCLASSIFIED RSRE-80006 DRIC-BR-75034 NL

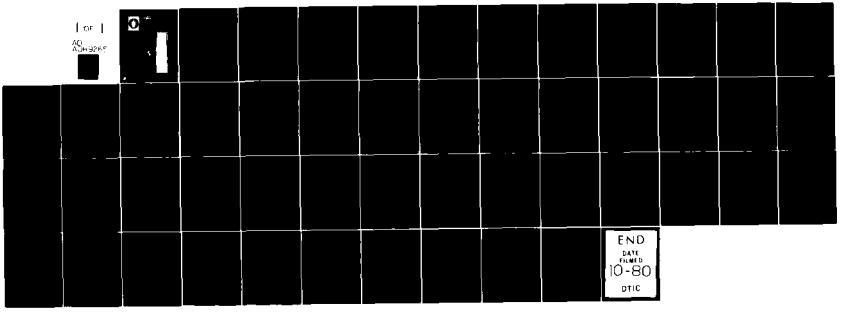

END
DATE FILMED
10-80
DTIC

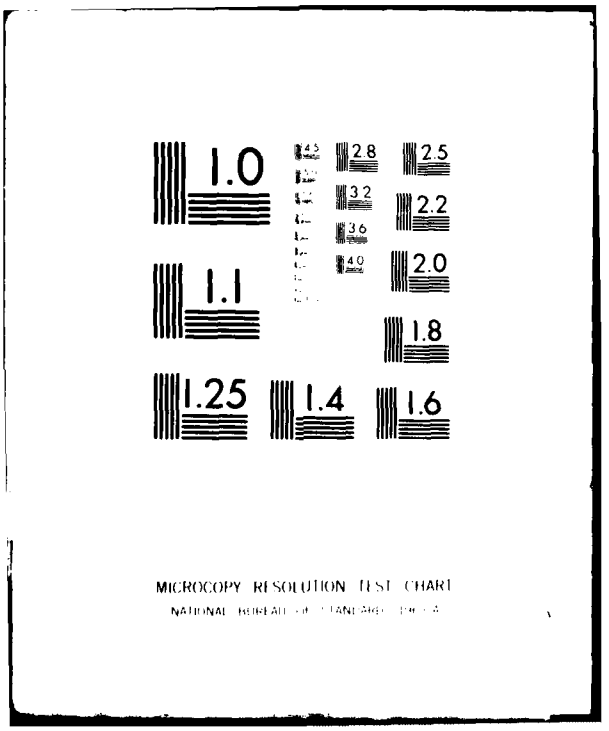
1.0
1.1
1.25
1.4
1.6
1.8
2.0
2.2
2.5
2.8
3.2
3.6
4.0
MICROCOPY RESOLUTION TEST CHART

UNLIMITED

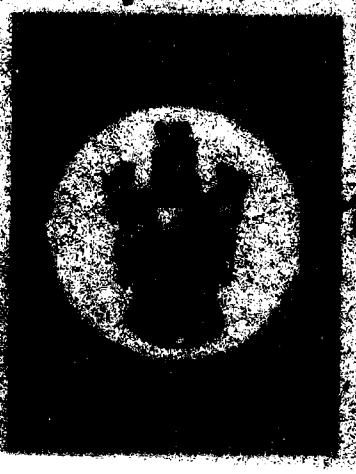

LEVEL

(2)

PROCUREMENT EXECUTIVE, MINISTRY OF DEFENCE
ROYAL SIGNALS AND RADAR ESTABLISHMENT, MALVERN

REPORT No. 80006

(6)

TITLE: DEVELOPMENTS IN UNITED KINGDOM WAVEGUIDE POWER STANDARDS

(10) ~~AUTHOR:~~ P. J. Skilton

DATE: April 1980

(11) Apr 80 (12) 32

(13) DRIC

(19) EF-75037

(14) RSRE-80006

SUMMARY

The United Kingdom national standards for power in waveguide consist of bolometer mounts of known efficiency at discrete frequencies from 8.2 GHz to 35 GHz. This report outlines recent developments in the design, construction, calibration and use of the standards. An analysis of random and systematic uncertainties in the microcalorimeter method of calibration forms a significant part of the report and yields an overall uncertainty of ± 0.1% in the mount efficiency with 95% confidence. Features of a technique for calibrating power meters in terms of a bolometer standard using a waveguide transfer instrument are described together with an analysis of uncertainty in the technique. Comparisons in the past five years of the RSRE developed standards with other power standards are also summarised.

401991 21

CONTENTS

1 INTRODUCTION

The microwave standards division at RSRE Malvern exists to provide national standards for rf and microwave quantities for the United Kingdom. This work is part of the programme of the Division of Electrical Science at the National Physical Laboratory (NPL). Since 1969 traceability for microwave attenuation, impedance, noise and power has been provided under the auspices of the British Calibration Service for the calibration laboratories of the Services Electronic Standards Centre (EQD-Aquila).

RSRE Technical Note 772 [1] described some of the early work at RSRE to provide waveguide power standards in X-band. The present report outlines the principal developments in the design, calibration and use of waveguide power standards at X-, J- and Q-band during the past four years. Random and systematic uncertainties associated with the automated calibration of standards and their transfer to waveguide or coaxial line travelling standards are quantified.

Some results of national and international inter-laboratory comparisons of power are described.

Bolometric standards exist at the frequencies [2,3] and in the waveguide sizes listed below:-

WG16	at	8.2 GHz
WG16	at	9.0 GHz
WG16	at	10.0 GHz
WG16	at	12.4 GHz
WG18	at	12.4 GHz
WG18	at	13.5 GHz
WG18	at	15.0 GHz
WG18	at	17.5 GHz
WG22	at	35.0 GHz

2 THE BOLOMETER AS A MICROWAVE POWER SENSOR

All waveguide power standards developed at RSRE utilise commercial Wollaston wire bolometer elements in waveguide mounts of RSRE design. (Wollaston wire is silver plated platinum drawn to the required diameter of the platinum core, typically two micrometres, and etched to remove the silver). The element forms one arm of a self-balancing Wheatstone bridge, the other three arms being high stability 200 Ω wirewound resistors (0.005% tolerance). When microwave power

is absorbed in the element its temperature and resistance increase and the dc dissipation in the element is reduced to maintain the bridge balance. In the circuit of fig 1 the dc substituted power in the element can be equated with the change in dc power in the opposite arm of the bridge. R_L represents the resistance of the lead from the bolometer to the bridge. To compensate for a voltage drop across this lead a similar voltage drop is produced in the opposite arm of the bridge by use of screened 4-core cable with the compensating leads shorted close to the bolometer. This configuration of the bridge only requires a single measurement of bridge resistance to characterise the bridge for use with any 4-core lead; it leaves the bolometer mount near earth potential and yields bridge voltages with respect to earth. (NB: If the bolometer mount was connected to waveguide at earth potential one part of the lead resistance would be shorted and the compensation would be in error by, typically 40 mΩ in 200Ω, ie 0.02%. It would however be normal practice to separate the bolometer mount from the adjoining waveguide by a dc block).

$$\text{DC SUBSTITUTED POWER} = \frac{V_0^2 - V_1^2}{200}$$

$$\text{EFFECTIVE EFFICIENCY} = \frac{\text{DC SUBSTITUTED POWER IN ELEMENT}}{\text{TOTAL MICROWAVE POWER ABSORBED IN MOUNT AND ELEMENT}}$$

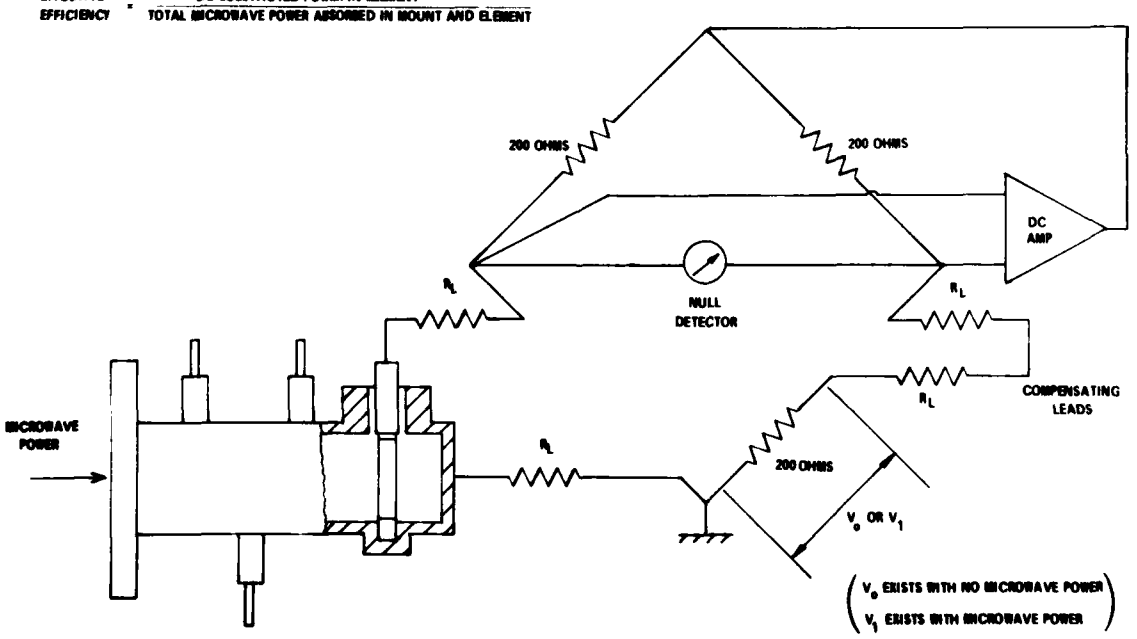

Figure 1 Self balancing bolometer bridge.

The dc substituted power is always less than the microwave power incident on the bolometer mount since it can only be equated with power absorbed in the element. Incident power dissipated in the mount itself, or reflected or leaked from the mount will not contribute to the dc substituted power. Thus a requisite in the design of a bolometer mount is the minimisation of reflected and leakage power as described in section 3, and quantifying incident power requires a knowledge of the mount effective efficiency, defined as the ratio of dc substituted power in the element to the total microwave power absorbed by the mount and element; the subject of section 4.

3 BOLOMETER MOUNT DESIGN

Fig 2 shows a cross-section typical of any of our recently developed X- or J-band standards. To maximise the efficiency of the mount it is electroformed in copper around a polished, stainless steel mandrel. This enables fine tolerances and a good surface finish to be achieved on the inside of the mount and also produces good electrical continuity between the short circuit terminating the mount and the waveguide walls. The mounts are designed for single frequency operation and the bolometer element is situated a quarter of a guide wavelength away from the short circuit.

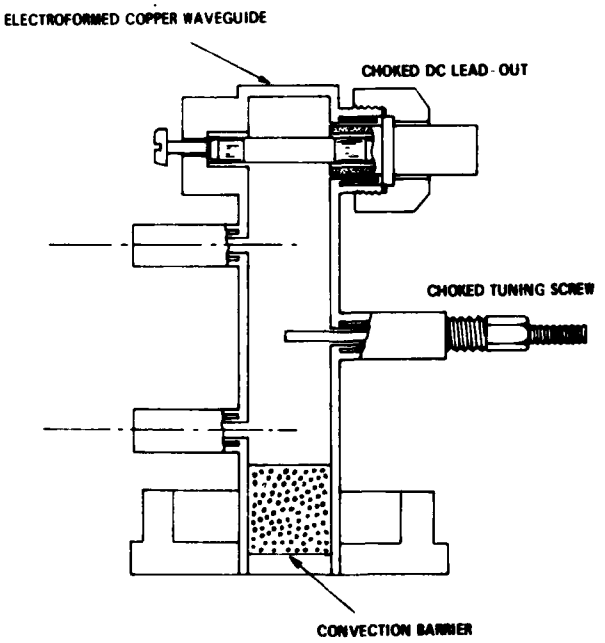

Figure 2. Waveguide bolometer mount

The dc lead-out from the element is surrounded by a half-wavelength, folded, air-spaced coaxial choke. A silver-copper eutectic bond is formed at a low impedance point between the inner and outer choke components. Similar chokes around the tuning screws reduce microwave leakage and provide smooth tuning of the mount by reducing the effect of variable dc resistance between the thread and mount body. Choking the dc lead-out and tuning screws results in a leakage signal of between 50 dB and 75 dB below the incident power. (Leakage measurements are made using a waveguide horn and a tuned spectrum analyser calibrated for power measurement with respect to a thermoelectric power meter at 1 μW).

The lockable and choked tuning screws, 0.5 mm diameter, reduce the voltage reflection coefficient of the mount to less than 0.01 at its design frequency resulting in a power loss of less than 0.01% due to reflection. Although these are still nominally single frequency devices, the VSWR of this design of mount remains less than 1.02 for typically ± 120 MHz.

A convection barrier of low loss dielectric foam is inserted in the entrance of the mount to prevent circulating air currents around the element and the mounts are gold plated. The plating minimises thermal radiation from the mount during calibration in a microcalorimeter (section 6.2) and prevents oxidisation of the copper which could cause a reduction in efficiency with age.

To minimise the risk of rotating the dc lead-out once the mount is assembled, the dc connection to the element is made through a bulkhead connector on the side of the mount. The lead-out which is potentially one of the most vulnerable parts of the mount, appears very robust and hence very stable, making these devices suitable for inter-laboratory travelling standards. Two calibrated 15 GHz bolometer mounts of this design were submitted in December 1978 as travelling standards in a WG18 international waveguide power comparison. In the course of the comparison they will be circulated to five North American and West European standards laboratories.

4 BOLOMETER MOUNT CALIBRATION USING A MICROCALORIMETER

4.1. The Calibration Method

Having produced a well matched and stable standard with low microwave leakage, its effective efficiency must be determined before it is capable of absolute power measurement. Since microwave power will be dissipated in the waveguide walls of the mount, in the tuning screws, the microwave chokes and the dielectric sheath enclosing the element the dc substituted power will

always be less than the microwave power incident on the mount. The principal method used at RSRE to measure the effective efficiency of a bolometric standard, involves measuring the microwave power absorbed in the element and, simultaneously, the power absorbed in the remainder of the mount. Power absorbed in the mount will manifest itself as an increase in mount temperature. Since the standards operate at a nominal 10 mW level, a mount whose efficiency is 98% will dissipate only 0.2 mW in the body of the mount and this would produce a temperature rise of less than 1m ^{o}C. To accurately measure such a small temperature change a very stable thermal environment is required for the standard.

To provide this stable environment, the mount is put in a twin jacket microcalorimeter and this calorimeter is immersed in a 170 litre water bath whose temperature is controlled to within ± 50μ ^{o}C per hour [4,5]. A simplified sectional view of a microcalorimeter is shown in fig 3. This is a development of a microcalorimeter design described by Engen [6], and originally copied

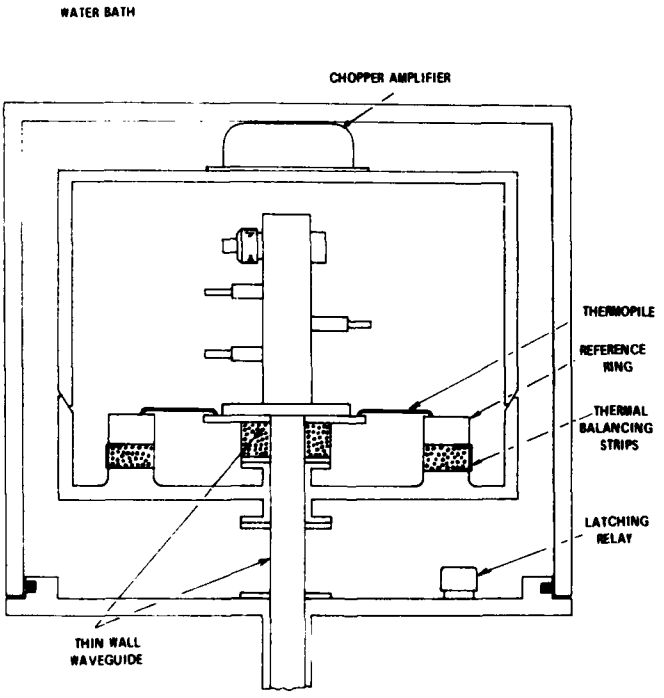

Fig 3. Microcalorimeter

at RSRE [1], which utilised two bolometers; one under calibration and the second acting as a temperature reference. The mount under calibration is inside the inner jacket and isolated from it by a length of thin wall copper waveguide.

Similarly, the inner and outer jackets are separated by another section of thin wall waveguide. The temperature of the mount flange is sensed by six chromel-constantan thermopiles between the flange and a reference ring around the mount. (This reference ring fulfils the same function as the second bolometer in Engen's microcalorimeter [6]). The thermal circuit of the calorimeter is balanced so that temperature fluctuations outside the calorimeter produce an equal effect at the bolometer flange and at the reference ring, thus minimising the effect of water bath temperature changes on the thermopile output. This balance is achieved by varying the number and thickness of copper strips to adjust the thermal path to the reference ring.

The output of the thermopiles, which is typically 100 μV, is amplified using a low noise chopper dc amplifier * which is in good thermal contact with the inner calorimeter jacket. This has removed the effect of laboratory temperature fluctuations on the amplified thermopile voltage and resulted in an order of magnitude reduction in random uncertainty when compared with an earlier situation where an expensive, high quality chopper amplifier was used outside the water bath to amplify the 100 μV from the microcalorimeter. A mercury wetted latching relay is used to short circuit the amplifier input, enabling remote adjustment of the amplifier offset voltage.

4.2 Example of a Mount Calibration

A trace of thermopile and bridge voltage resulting from the calibration of a 98% efficient X-band mount is shown in fig 4. With only dc bias on the bolometer, the 15 mW dissipation raises the temperature of the bolometer mount flange by about 60m ^{o}C giving an output from the thermopiles of approximately 120 μV. When 10 mW of microwave power is incident on the mount, the dc bias is reduced to maintain the dissipation in the element. However, the dissipation in the mount body raises the temperature by a further 0.7 m ^{o}C increasing the thermopile output by approximately 1.3 μV. The uncertainty in measuring the output from the thermopile amplifier is less than ± 40 nanovolts (referred to the input) arising mainly from noise generated at the thermojunction. (The topic of random uncertainty is fully discussed in 6.1). Clearly, the more efficient the mount the smaller the temperature rise on application of microwave power. During a full 24 hour calibration microwave power is incident on the mount for alternate one hour periods. At the end of each one hour period the frequency bridge voltage and thermopile output are recorded automatically. This method of calibration consistently yields random uncertainties of between ± 0.02% and ± 0.06% (95% confidence limits) from sets of 12 results in a 24 hour period.

* Ancom model 15C-3a, Ancom Ltd, Cheltenham, England.

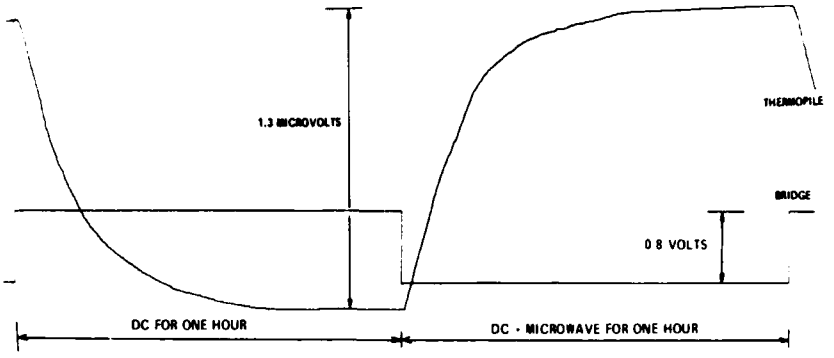

Figure 4. Variation in thermopile and bridge outputs when calibrating a 98% efficient mount.

4.3 Computer Controlled Calibration

An automated method of bolometer mount calibration has been in use at RSRE since 1974 [7]. The method has recently been extended and fig 5 illustrates the principal items used in a computer controlled microcalorimeter measurement of mount efficiency. V_o and V_1 represent the dc voltages present on the self-balancing bridge under conditions of no microwave power and with microwave power on the mount; e_o and e_1 represent the amplified thermopile voltages under

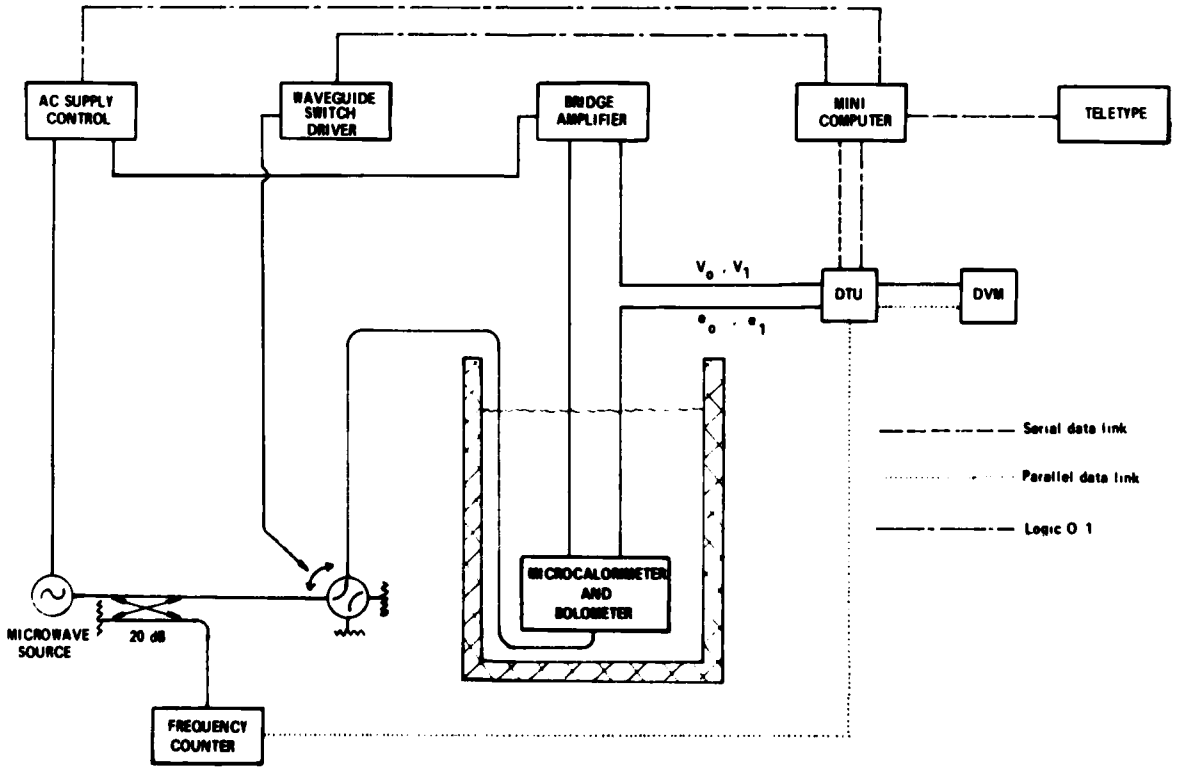

Fig 5. Apparatus for a computer controlled calibration

the same conditions. The start of the calibration can be delayed until thermal stability in the microcalorimeter is indicated by a declining drift rate in the bridge and thermopile voltages with dc dissipation only in the bolometer. Thereafter at 60 minute intervals the computer initiates a scan of the bridge and thermopile voltages and operates the waveguide switch. After three hours sufficient data has been stored to enable the result of one measurement of mount efficiency to be calculated. The calibration ends when the number and the standard deviation of results fulfil program limits. The thermal offset voltage is the output from the thermopile with no microwave or dc dissipation in the mount and has proved to be constant for a given design of mount. Offsets in excess of 1 μV at the thermopile amplifier input create a significant systematic uncertainty in the efficiency calibration - see 6.2. At the end of the efficiency measurement the microwave source and bridge are switched off and the thermal offset voltage is recorded. The choice of switching period, real-time result processing, facilities for checking on the progress of a calibration and removing the need for an operator at the start and end of a calibration are the principal benefits of a computer controlled method.

5 THEORY OF A MICROCALORIMETER CALIBRATION

The theory of the calibration and subsequent analysis of uncertainty have been documented in the following order:-

i) the full theory of a calibration using, necessarily, imperfect equipment (Section 5)

ii) simplified to the theory of a calibration with perfect equipment (Section 5)

iii) followed by an assessment of uncertainty incurred in assuming a perfect calibration (Sections 6.2 to 6.4).

Quantifying each imperfection in the calibration process as a systematic correction to be applied to the result of an otherwise perfect calibration has the following advantages:-

i) the perfect calibration requires no piece of data which depends on the microcalorimeter and the mount geometry

ii) for a given microcalorimeter and mount geometry the systematic corrections remain virtually constant.

A brief qualitative description of the imperfections present in a microcalorimeter calibration will assist in defining terms. Fig 6, which is not to scale, illustrates the relationship between the output of the thermopile amplifier and power dissipated in the bolometer during a calibration. With no dissipation in the bolometer a small offset voltage is present at the

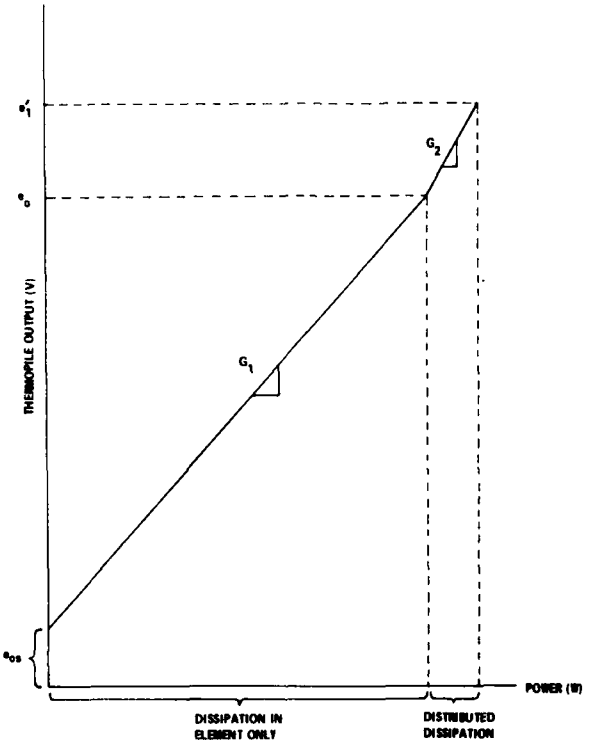

Figure 6. Thermopile amplifier output as a function of power dissipation in the bolometer mount.

output of the thermopile amplifier (e_{os}); this arises from thermal imbalance in the microcalorimeter (Section 6.2). Biasing the bolometer to its operating resistance causes the thermopile output to increase linearly to e_o. The sensitivity of the thermopile to dissipation at the bolometer is denoted by G_1 (VW^{-1})-see fig 6. On applying microwave power it has been assumed that the sensitivity of the thermopiles to microwave and dc dissipation in the element remains at G_1 but that the sensitivity to the typically 1% to 3% of microwave power lost in the mount changes to G_2 (VW^{-1}) (Section 6.3). In addition to microwave dissipation in the mount, there will also be dissipation in the waveguide preceding the mount flange and this will contribute to the thermopile output. Section 6.4 describes how this contribution can be quantified. (e_1' in fig 6 is assumed to have been corrected for the effects of input waveguide heating, ie e_1' is the value of thermopile output associated only with microwave dissipation in the mount).

With the bolometer element biased as shown in fig 1 and no microwave power on the mount the dc dissipation will be:-

$$\frac{V_o^2}{R} = \frac{(e_o - e_{os})}{G_1} \tag{1}$$

where R is the operating resistance (in ohms) of the element. When microwave power is applied the total power dissipated in the mount, P_{tot}, will be:-

$$P_{tot} = \frac{(e_o - e_{os})}{G_1} + \frac{(e_1' - e_o)}{G_2} \tag{2}$$

and the dc power in the element is $\frac{V_1^2}{R}$.

Hence microwave power in the mount, P_{mw}, will be:-

$$P_{mw} = P_{tot} - \frac{V_1^2}{R} \tag{3}$$

From (1) and (2)

$$P_{tot} = \frac{V_o^2}{R} \left\{ 1 + \frac{G_1}{G_2} \left(\frac{e_1' - e_o}{e_o - e_{os}} \right) \right\} \tag{4}$$

$\therefore$ from (3)

$$P_{mw} = \frac{1}{R} \left[V_o^2 \left\{ 1 + \frac{G_1}{G_2} \left(\frac{e_1' - e_o}{e_o - e_{os}} \right) \right\} - V_1^2 \right] \tag{5}$$

Since the effective efficiency of the mount is defined as:-

$$\eta_e = \frac{\text{dc substituted power in element}}{\text{total microwave power absorbed in mount and element}}$$

equation (5) with the expression for dc substituted power yields:-

$$\eta_e = \frac{1 - \left(\frac{V_1}{V_o} \right)^2}{\left\{ 1 + \frac{G_1}{G_2} \left(\frac{e_1' - e_o}{e_o - e_{os}} \right) \right\} - \left(\frac{V_1}{V_o} \right)^2} \tag{6}$$

Now e_1' can be derived from the measured value of thermopile voltage (e_1) and a prior knowledge of the sensitivity of the thermopiles to dissipation in the waveguide preceding the mount flange (δ, VW^{-1}), as follows:-

$$e_1 = e_1' + \delta\left(\frac{V_o^2 - V_1^2}{\eta_e R}\right) \tag{7}$$

the term in brackets on the right hand side of (7) being the microwave power absorbed by the matched mount. Substituting (7) in (6) yields η_e explicitly as:-

$$\eta_e = \frac{1 - \left(\frac{V_1}{V_o}\right)^2 + \frac{G_1}{G_2}\left(\frac{V_o^2 - V_1^2}{e_o - e_{os}}\right)\frac{\delta}{R}}{1 - \left(\frac{V_1}{V_o}\right)^2 + \frac{G_1}{G_2}\left(\frac{e_1 - e_o}{e_o - e_{os}}\right)} \tag{8}$$

From (8) four significant special cases can be derived:-

i) when $G_1 = G_2$ and $e_{os} = \delta = 0$, ie a perfect calibration in which all of the three imperfections outlined above are absent. (8) reduces to:-

$$\eta_e = \frac{1 - \left(\frac{V_1}{V_o}\right)^2}{\frac{e_1}{e_o} - \left(\frac{V_1}{V_o}\right)^2} \tag{9}$$

ii) when $G_1 = G_2$ and $e_{os} = 0$, ie considering only the effect of input waveguide heating on a perfect calibration. (8) reduces to:-

$$\eta_e = \frac{1 - \left(\frac{V_1}{V_o}\right)^2 + \left(\frac{V_o^2 - V_1^2}{e_o}\right)\frac{\delta}{R}}{\frac{e_1}{e_o} - \left(\frac{V_1}{V_o}\right)^2} \tag{10}$$

iii) when $G_1 = G_2$ and $\delta = 0$, ie considering only the effect of thermopile offset voltage on a perfect calibration. (8) reduces to:-

$$\eta_e = \frac{1 - \left(\frac{V_1}{V_o}\right)^2}{1 - \left(\frac{V_1}{V_o}\right)^2 + \left(\frac{e_1 - e_o}{e_o - e_{os}}\right)} \qquad (11)$$

iv) when $\delta = 0$ and $e_{os} = 0$, ie considering only the effect of a change in the thermopile sensitivity between dc heating of the mount and dc plus microwave heating. (8) reduces to:-

$$\eta_e = \frac{1 - \left(\frac{V_1}{V_o}\right)^2}{1 - \left(\frac{V_1}{V_o}\right)^2 + \frac{G_1}{G_2}\left(\frac{e_1}{e_o} - 1\right)} \qquad (12)$$

6 UNCERTAINTY IN A MICROCALORIMETER CALIBRATION

The total uncertainty in the calibration is most conveniently derived by consideration of its components. These comprise the random uncertainty and four sources of systematic uncertainty. Since a small random component of uncertainty facilitates the resolution of systematic uncertainties, the estimation of random uncertainty is discussed first.

6.1 Random Uncertainty

This has been derived from the specified or experimentally observed performance of each piece of apparatus used in the calibration. Such a derivation can yield the relative importance of individual contributions to the random uncertainty enabling efforts to reduce the uncertainty to be appropriately directed. In deriving the random uncertainty associated with the microcalorimeter determination of bolometer mount efficiency, contributions from the following effects were quantified:-

i) thermopile and thermopile amplifier noise. The uncertainty associated with e_o and e_1 was assumed to have a Gaussian probability distribution and after monitoring e_o and e_1 the 95% limits of this distribution were estimated to be ± 0.03% (± 40 nanovolts in approximately 120 microvolts referred to the amplifier input). This noise originated predominantly in the thermojunctions; the amplifier alone contributing less than one third of the above figure.

ii) uncertainty in voltage measurement. Since the random uncertainty being evaluated was that associated with a 24 hour calibration the uncertainty arising from voltage measurement was derived using the 24 hour specification for the dvm. That is:-

$\pm$ (0.00015% V_o + 0.0001% of 10 Volts) for V_o and V_1
and $\pm$ (0.0004% e_o + 0.00015% of 1 Volt) for e_o and e_1

These were assumed to be rectangular limits.

iii) bridge and bridge amplifier noise. The noise voltage superimposed on V_o was observed to be typically 5 μV peak-to-peak in 1.7V so 95% limits of the Gaussian distribution associated with V_o were set as $\pm$ 0.00015%.

iv) microwave power instability. A change in the microwave power level immediately prior to recording V_1 and e_1 would produce an uncertainty in the calculated value of efficiency since V_1 would respond to the change in a few milliseconds whereas e_1 would take several minutes to follow. Assuming power level changes as large as $\pm$ 0.5% were occurring, these would only result in an uncertainty in efficiency of $\pm$ 0.007%. (In practice the performance of the source is much better than this but the preceding figures show that particular care in levelling the source is not essential).

The effect of each of these uncertainties on the calculated value of efficiency was determined using equation (9). Mean values of V_o, V_1, e_o and e_1 derived from averaging dvm readings, as in a real calibration, were varied about a typical measured value by random selection from the appropriate Gaussian or rectangular distribution and substituted in (9). Equation (9) was evaluated 200 times for each of the sources of uncertainty previously listed as (i) to (iii) and the 95% confidence limits (95% CL) of the resulting distribution of efficiency values were determined. The results of this exercise are shown in Table 1 and the total uncertainty derived following the recommendations of reference 8.

Component of uncertainty	Magnitude & distribution
Thermopile/amplifier noise	± 0.041% (95%, Gaussian)
Voltage measurement	± 0.001% (95%, Gaussian)
Bridge/amplifier noise	< ± 0.001% (95%, Caussian)
Power instability	± 0.007% (95%, Gaussian)
Total	± 0.047% (95% CL)

TABLE 1 COMPONENTS OF RANDOM UNCERTAINTY

NB: Total uncertainty $= \pm 1.96 \left\{ \frac{0.041}{2} + \left[\left(\frac{0.001}{2} \right)^2 + \left(\frac{0.007}{2} \right)^2 \right]^{\frac{1}{2}} \right\}$

The microwave power level at which the calibration is performed will have a significant effect on the magnitude of the thermopile noise contribution; increasing the power level will reduce the influence of thermopile noise. The value of ± 0.041% in Table 1 assumes a power level during calibration of 8 mW; the minimum likely to be encountered.

During an eight month period in 1979 the observed mean 95% confidence limits associated with 30 calibrations of 22 X- and J-band mounts, with efficiencies greater than 97%, were ± 0.043%. Such a result increases confidence in the uncertainty analysis and provides a clear indication of whether a calibration is under experimental control; an unstable mount or malfunction of the water bath control, for example, being clearly evident. When comparing results between calibrations, rather than within a calibration, a significant source of random uncertainty that must be considered is that associated with the repeatability of the waveguide flanged coupling to the microcalorimeter.

6.2 Systematic Uncertainty Arising From Thermal Offset

The thermal offset voltage has been defined as the output from the thermopile amplifier with zero dissipation in the bolometer mount. It is a function of the number and cross-section area of the copper straps between the reference

ring and inner jacket of the microcalorimeter (fig 3), dissipation in the chopper amplifier (up to 100 mW) and the mount under calibration. Observations at J- and Q-band have shown that, for gold plated mounts, the offset voltage is a function of surface area; the measurement flange temperature increasing as the mount is changed for one of larger surface area. With zero dissipation in the mount, energising the thermopile amplifier raises the temperature of the inner microcalorimeter jacket and causes the mount to absorb heat from its warmer surroundings; the amount of heat absorbed depending on the area of the surface and its absorption coefficient. To further investigate this effect a low efficiency, gold plated Q-band mount was coated in matt black paint, increasing the absorption coefficient/emissivity of the surface. A change of 10% was observed in the offset voltage indicating a temperature increase at the flange and confirming the significance of heat transfer by radiation on the magnitude of this voltage *.

Eliminating convection currents within the inner jacket of the J-band microcalorimeter by placing loosely packed cotton-wool around the mount produced a change of approximately 10% in the offset voltage indicating a reduction in temperature at the measurement flange ≠.

In practice it has proved easier to produce an approximate thermal balance in the microcalorimeter using copper straps, then to monitor the offset voltage for each calibration and use (11) to correct the result of (9). A typical

---

* A subsequent calibration of the blackened Q-band mount with corrections applied for input waveguide heating and thermopile offset peculiar to that mount, yielded a result of 0.1% higher than before painting. During a calibration the temperature of the mount is higher than its surroundings and radiation from the black mount surface is greater than that from the former gold surface resulting in an optimistic value of efficiency. These results offer an explanation of the variation in offset voltage between mounts, illustrating the need to measure offset for each configuration of mount encountered, and provide further justification for gold plating mounts since the assumption is made that radiative heat loss during a calibration is insignificant.

≠ In addition to influencing the offset voltage the presence of convection currents can directly affect the measured value of efficiency. Eg at J-band the effect of reducing convective cooling by surrounding the mount with a convection barrier is < 0.02% for a 98.8% efficient mount.

correction to the result of (9) obtained with a 98.8% efficient J-band mount is + 0.032% ± 0.0006% (95% CL).

6.3 Systematic Uncertainty Arising From Thermopile Sensitivity Variation

Power dissipated in the bolometer element raises the temperature of the surrounding mount and once thermal equilibrium is attained this temperature increase is recorded by thermopiles at the flange of the microcalorimeter, some 60 to 90 mm away from the source of dissipation. With microwave power incident on the mount typically 1 to 3% of the power absorbed is distributed throughout the mount. Since, under conditions of constant dissipation the mount attains thermal equilibrium there must be some heat loss from the mount. This produces temperature gradients along the mount and consequently the thermopile output becomes a function of both the dissipation within the mount and position at which that dissipation occurs. An experiment was devised to substitute the distributed microwave power with distributed dc power, which could be accurately measured, and hence quantify any change in the sensitivity of the thermopiles between localised heating, at the element, and distributed heating.

Having determined the efficiency of a mount using (9), an auxiliary heater, assembled from six 1/8 W 1 kΩ resistors connected in series, was placed around the outside of the mount. The heater was in good thermal contact with the mount and covered with polished copper foil to minimise radiation. A convection barrier of loosely packed cotton wool was put around the mount. A check of efficiency revealed no significant difference resulting from the addition of the heater. With a constant dc bias on the bolometer element current was switched to the auxiliary heater for alternate one hour periods and the heater and thermopile output recorded for bias currents ranging from 105 μA to 175 μA. This range of dissipation was equivalent to mount efficiencies from 99.5% to 98.7%. For a particular J-band mount the resulting values of G_1 and G_2 (-43.705 ± 0.015 VW^{-1} and -44.810 ± 0.240 VW^{-1} respectively) used in (12) yield a correction of + 0.032% ± 0.007% (95% CL) for a mount of 98.8% efficiency.

Clearly it is not practical to fit an auxiliary heater around every mount requiring calibration but the results obtained with one mount can be applied using (12), to others of the same design. It can be seen from fig 6 that the

correction to the thermopile voltage is proportional to the loss in the mount; in the previous example the correction reduces e_1 by 2.5%.

Similar corrections for the enhancement of the thermopile output during microwave heating have been reported. Using two discrete dc heaters inside the mount estimates of the reduction to be made to the thermopile output vary from 1%[6] to 2.4%[9] and using two flat dc heating coils inside the mount a reduction of 2% was estimated [9].

6.4 Systematic Uncertainty Arising From Input Waveguide Heating

When microwave power is incident on a dc biased mount at the measurement flange of a microcalorimeter, the thermopile output will increase because of microwave dissipation in the mount. The waveguide preceding the mount possesses finite microwave attenuation and dissipation occurring in this waveguide will contribute to the thermopile output. For every microcalorimeter it is necessary to determine the sensitivity of the thermopiles to input waveguide heating. Since the contribution to the thermopile output arising from heating of the input waveguide cannot be separated from the contribution arising from heating a matched termination at the microcalorimeter flange, the matched termination is replaced by a short circuit. An allowance can be made for dissipation in the short circuit but the principal contribution to the thermopile output will now arise from dissipation in the input waveguide. In practice the short circuit consists of a piece of polished copper foil across the flanged joint between the bolometer mount and the microcalorimeter. Since the sensitivity of the thermopiles to input waveguide heating is a function of the device at the measurement flange, this method of producing an electrical short circuit does not alter the thermal circuit encountered during a calibration.

Once the sensitivity of the thermopiles to input waveguide heating has been determined with a short circuit at the measurement plane these results have to be related to the thermopile sensitivity when the short circuit is replaced by a well matched bolometer mount. The ratio of dissipation over a length of input waveguide ($z = \ell_1$, to $z = \ell_2$) terminated at the measurement flange ($z = o$) in a short circuit, to dissipation over the same length with a mount of voltage reflection coefficient Γ_L at $z = o$ is calculated in Appendix A.

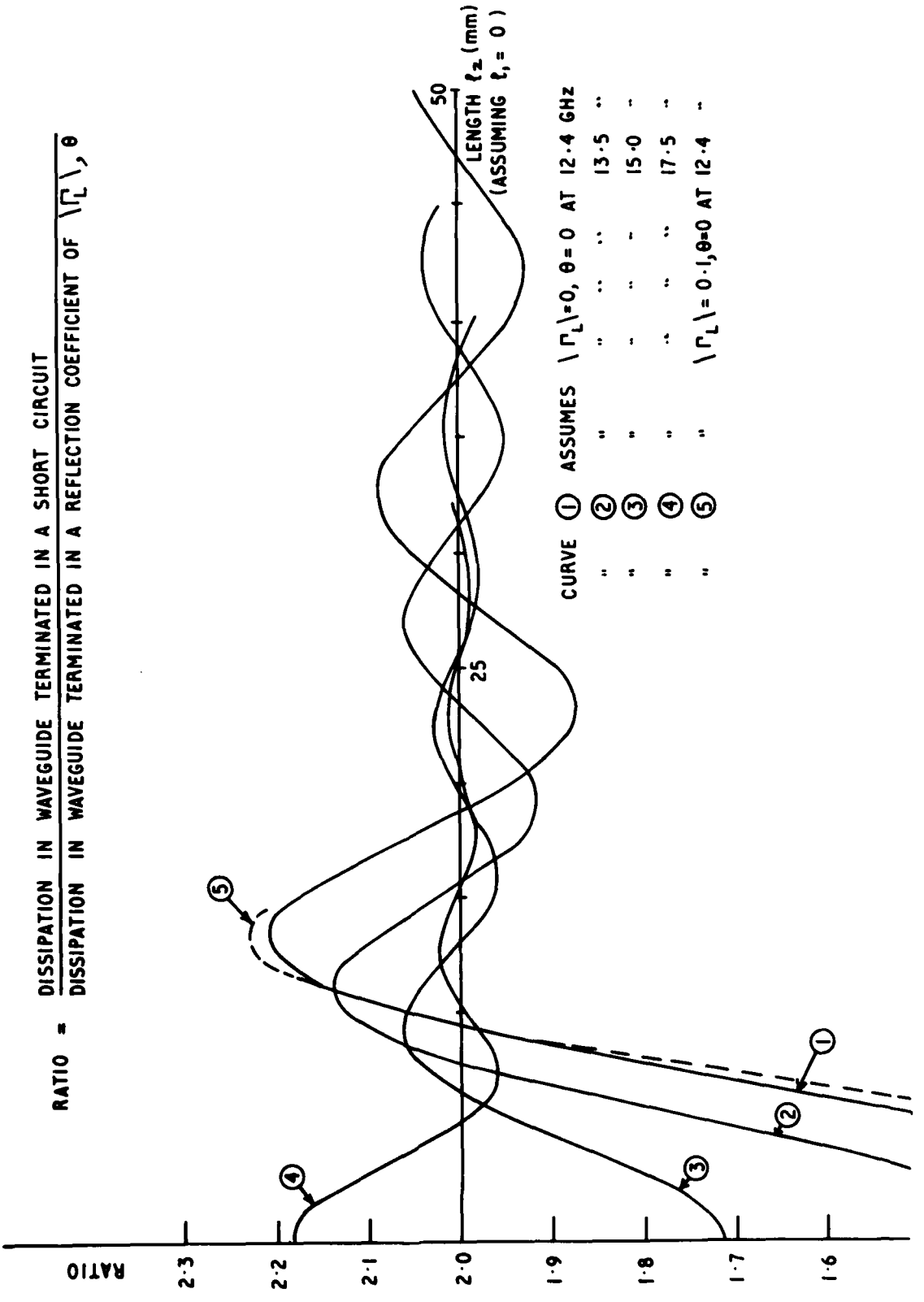

Fig 7 Ratio of input waveguide heating as a function of waveguide length for a WG18 microcalorimeter.

Fig 7 illustrates the dependence of this ratio on frequencies in the WG18 band and on the length of waveguide (ℓ_2) over which dissipation occurs. If the waveguide preceding the measurement flange has a uniform attenuation constant then at all frequencies the ratio will tend to 2. The techniques used to fabricate the 15 mm long thin wall thermal isolation section preceding the measurement flange in the RSRE WG18 microcalorimeter have resulted in a relatively poor internal surface finish. The effect of 15 mm of lossy waveguide preceding the flange results in ratios of dissipation tending towards the values in fig 7, ie 2.18 at 12.4 GHz, 2.03 at 13.5 GHz, 1.97 at 15 GHz and 2.00 at 17.5 GHz. Similarly, high attenuation at a poor flanged joint or waveguide window will affect the thermopile response when their sensitivity, measured in the presence of a short circuit, is used to predict their sensitivity when the short is removed. For example, assuming high dissipation in the input waveguide between ℓ_1 = 59 mm and ℓ_2 = 59.5 mm and a matched mount, then using (A 24) the ratios of heating effect will tend to 1.47 at 12.4 GHz, 1.82 at 13.5 GHz, 2.24 at 15 GHz and 2.07 at 17.5 GHz.

Unless the profile of attenuation constant along the input waveguide is known, the results of Appendix A will only be an approximation to the real situation. However, the results illustrate the need for uniformity over the input waveguide if the thermopile sensitivity determined with a short circuit at the measurement flange is to be simply related to the thermopile sensitivity when a bolometer is under calibration.

With a matched 15 GHz bolometer mount under calibration the sensitivity of the RSRE WG18 microcalorimeter to input waveguide heating is 0.029 ± 0.002 VW^{-1} The uncertainty arises from that in measuring the thermopile output with a short circuit preceding the bolometer and uncertainty in the ratio of heating effects. For a 98.8% efficient mount equation (10) results in a correction to (9) of + 0.067% ± 0.005% (95% CL).

6.5 Systematic Uncertainty Arising From RF-DC Substitution

The difference in thermopile sensitivity between localised dc heating of the mount (at the element) and localised plus distributed heating with microwave power incident on the mount has been quantified in 6.3. The rf-dc substitution error discussed in this section arises from the different current distributions in the bolometer element with dc heating and with microwave heating. If a substitution error exists then the dc power required to bias the element to a resistance of 200 ohms, for example, would not equal the microwave power required to maintain 200 ohms.

Calculations have been made of the rf-dc substitution error in a bolometer element [10,11,12] and the latest of these [12] indicates that the substitution error is a function of waveguide size, frequency and the geometry of the element and its supports. For example, reproducing the result at 12.2 GHz in WG16, the substitution error will increase from 0.002% to 0.21% when the radius of the posts supporting the element decreases from 2.5 mm to 0.04 mm and the element dimensions remain unaltered.

One experimental determination [13] of substitution error compared the efficiency of a bolometer mount determined from a microcalorimeter with its efficiency determined by an impedance method [14]. (The latter technique regards the bolometer mount as a lossy two-port terminated in a resistive load; namely the element. The input reflection coefficient of the two-port is measured on a highly tuned reflectometer with the bolometer element biased successively to 160 ohms, 200 ohms and 240 ohms. Expressions for the three values of input reflection coefficient are solved simultaneously to yield the S-parameters of the two-port and hence the mount efficiency). The reported [13] differences in mount efficiency at X-band (microcalorimeter method - impedance method) vary from 0.14% at 8.2 GHz to 0.67% at 12.2 GHz with an estimated uncertainty of ± 0.7%. Values of efficiency at 10 GHz, typically 0.29% less than the microcalorimter values, were obtained in 1974 at RSRE when work on the impedance method was terminated.

There is however no evidence to suggest that this difference arose solely from a rf-dc substitution error. On the contrary, there is considerable evidence at X, J and Q-band that, for the RSRE standards, the substitution error is at least an order of magnitude less than the figure quoted above. If a significant error arose from equating the dc substituted power in a bolometer wire with the absorbed microwave power then it would manifest itself when a calibrated bolometer was compared with a non-bolometric standard (including a thermistor standard where the current distribution is likely to differ from that in a bolometer wire and a different value of substitution error could be expected). Evidence at present available from such comparisons (see Section 9) indicates that for the RSRE bolometric standards the rf-dc substitution error does not add significantly to the uncertainties summarised in 6.6. Reports from other standards laboratories [6,9,15] similarly indicate that no correction is required to compensate for rf-dc substitution error at X-band.

6.6 Overall Uncertainty

Three systematic uncertainties in a microcalorimeter bolometer mount calibration have been quantified in sections 6.2 to 6.4. The typical value quoted for each uncertainty is that associated with a 15 GHz laboratory standard bolometer (J 9). For this particular mount the overall systematic correction to the value resulting from (9) is derived in Table 2.

Correction for:-	Magnitude & 95% CL (%)
Thermal offset	+ 0.032 ± 0.001
Thermopile sensitivity	+ 0.032 ± 0.007
Waveguide heating	+ 0.067 ± 0.005
Total	+ 0.13 ± 0.01

TABLE 2 COMPONENTS OF SYSTEMATIC CORRECTION

The overall uncertainty will include the random uncertainty derived in 6.1, the uncertainty in the systematic correction and the uncertainty associated with the repeatability of the flanged connection to the microcalorimeter. A value of ± 0.02% (± 0.001 dB) has been assigned to this last uncertainty based on preliminary results at 17.5 GHz using a resonant cavity technique [16]. The overall uncertainty is derived in Table 3.

Component of Uncertainty	Magnitude (%)
Random	± 0.05
Systematic correction	± 0.01
Flange	± 0.02
Total	± 0.06

TABLE 3 COMPONENTS OF OVERALL UNCERTAINTY

Although not easily quantifiable it is known that other sources of uncertainty could add to this total. It is, for example, possible to resolve the effects of convective cooling of the mount within the microcalorimeter (< 0.02%) and there is the possibility of a small rf-dc substitution error. Results of the preceding uncertainty analysis and the confidence gained from the comparisons described in Section 9, indicate that for this standard and other low leakage stable mounts which have been evaluated as described in 6.2 to 6.4, a realistic uncertainty in their efficiency is ± 0.1% (95% CL).

7 POWER METER CALIBRATION USING A TRANSFER INSTRUMENT

The microcalorimeter and water bath method of measuring the effective efficiency of a bolometer mount has the advantage of being an absolute method but it also has disadvantages and some of these are listed on the left hand side of Table 4. A method of efficiency measurement which is considerably more versatile than the microcalorimeter, and which utilises the absolute value of efficiency determined with the microcalorimeter, involves the use of a waveguide transfer instrument [17] and, as can be seen from the right hand side of Table 4, it ideally complements the microcalorimeter.

	Micro-Calorimeter	WG Transfer Instrument
Is method absolute?	Yes *	No
How long for 12 results?	48 Hours	30 Mins
Devices other than Bolometers?	No	Yes
Does method allow for a 'leaky' mount?	No	Yes
Can method detect a mismatched mount?	No	Yes

* For leak-proof, matched mounts

TABLE 4 COMPARISON OF MICROCALORIMETER AND TRANSFER INSTRUMENT CALIBRATIONS.

The waveguide transfer instrument is basically a tuned reflectometer and is illustrated in a simplified form in Fig 8.

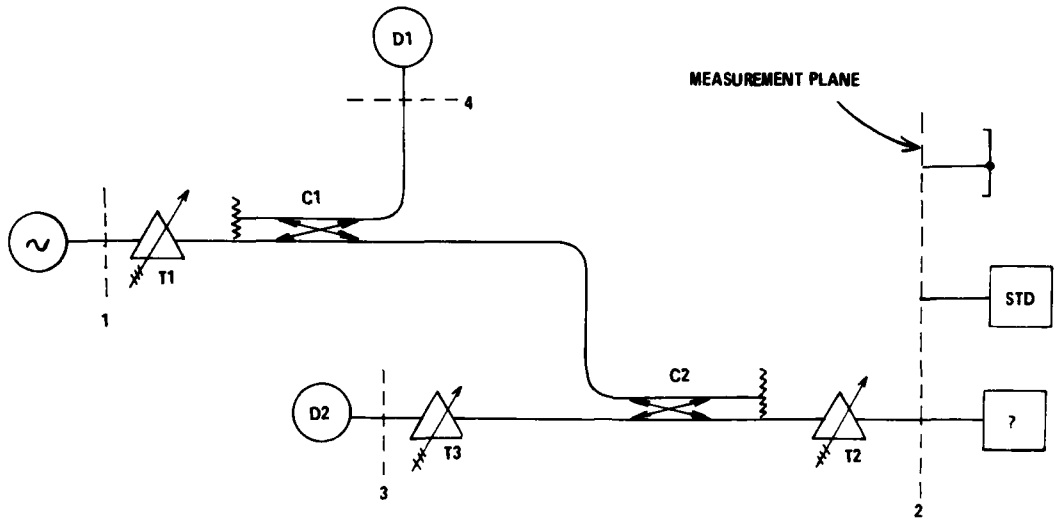

Figure 8. Transfer Instrument for Comparing Power Meters.

Imperfections in the directional couplers C1 and C2, are cancelled by the tuners T1, T2 and T3 such that detector D1 produces an output directly proportional to forward going power at the measurement plane and D2 produces an output directly proportional to power reflected from the device at the measurement plane. Once tuned, the instrument is calibrated, first with an offset short circuit at the measurement plane, noting the outputs of D1 and D2, then with a standard bolometer replacing the short, noting D1, D2 and the bolometer bridge voltage. The calibration constants of the transfer instrument together with the outputs from D1 and D2 enable the efficiency and voltage reflection coefficient of any other power sensor to be measured. With calibrated waveguide to coaxial line adaptors [18] at the measurement plane the transfer instrument can be used to measure the efficiency of coaxial line power meters (see section 9.2).

When the instrument is tuned the power absorbed by a termination at port 2 (P_2) is related to the power at ports 3 and 4 (P_3 and P_4) by:-

$$P_2 = K_1 P_4 - K_2 P_3 \tag{13}$$

where K_1 and K_2 are constants of the instrument. Terminating port 2 in a perfect short circuit will make $P_2 = 0$, giving:-

$$\frac{K_1}{K_2} = \left(\frac{P_3}{P_4} \right)_{sc} \tag{14}$$

Replacing the short circuit with a standard bolometer gives:-

$$(P_2)_{std} = K_1(P_4)_{std} - K_2(P_3)_{std} \tag{15}$$

and from (14) and (15) K_1 and K_2 are given by:-

$$K_1 = \frac{(P_2)_{std}}{(P_4)_{std} - \left(\frac{P_4}{P_3}\right)_{sc}(P_3)_{std}} \tag{16}$$

and

$$K_2 = \frac{(P_2)_{std}}{\left(\frac{P_3}{P_4}\right)_{sc}(P_4)_{std} - (P_3)_{std}} \tag{17}$$

With a power meter of unknown efficiency at the measurement plane of a calibrated transfer instrument the true power absorbed by the meter will be:-

$$K_1P_4 - K_2P_3$$

Assuming the indicated power to be $(P_2)_u$ then the efficiency of the power meter (η_u) will be:-

$$\eta_u = \frac{(P_2)_u}{K_1P_4 - K_2P_3} \tag{18}$$

The voltage reflection coefficient (vrc) of the power meter can be obtained from equation (14) and the power ratio between ports 3 and 4 with the unknown connected.

$$vrc = \left\{\left(\frac{P_3}{P_4}\right)_u \left(\frac{P_4}{P_3}\right)_{sc}\right\}^{\frac{1}{2}} \tag{19}$$

At RSRE transfer instruments have been assembled in waveguide sizes WG16, WG18 and WG22. Features common to all of them include:-

a) assembly of all waveguide components on a vertical aluminium casting to provide good thermal and mechanical stability.

b) RSRE designed and manufactured three screw tuners for T_1, T_2 and T_3. These are fitted with digital micrometers and broadband chokes to provide quick, smooth and accurate retuning of the instrument on changing frequency.

c) a motor driven waveguide switch following the microwave source. The drive unit for the switch is based on a Geneva mechanism and this ensures extremely smooth mechanical operation.

d) temperature control of the thermistor power meters at D_1 and D_2 to better than ± 2 m ^{o}C in a 3 minute period (the time required for one result) and similar temperature control at a water jacket preceding the measurement plane.

e) a sequence controller. This initiates voltage scans of power meter outputs, operates the waveguide switch driver and counts the number of measurement cycles up to a preset maximum.

f) a microwave source whose frequency is controlled to better than ± 5 kHz for the duration of a calibration.

8 UNCERTAINTY IN A TRANSFER INSTRUMENT MEASUREMENT

An analysis of the uncertainty in a transfer instrument calibration and its subsequent use to measure the efficiency (or calibration factor) of a power meter can be divided into three stages with the uncertainty in one stage carried forward to the next. The three stages are:-

a) uncertainty in $\frac{K_1}{K_2}$ (using a short circuit)

b) uncertainty in K_1 (using a standard bolometer)

c) uncertainty in η_u (an unknown efficiency termination).

Table 5 lists some sources of uncertainty and indicates which of the terms (a) to (c) are affected.

NB:- K_2 is determined from K_1 and the ratio $\frac{K_1}{K_2}$.

Source of Uncertainty	Affecting uncertainty in:-		
	$\frac{K_1}{K_2}$	K_1	Γ_u
Imperfect tuning of T1	✓	✓	✓
Imperfect tuning of T2	✓	✓	✓
Imperfect tuning of T3	✓	✓	✓
Mismatch of standard		✓	
Mismatch of unknown			✓
vrc of short circuit	✓		
Standard mount efficiency		✓	
Noise & drift in power meters	✓	✓	✓
Voltage measurement	✓	✓	✓
Variation in source power	✓	✓	✓
$\frac{K_1}{K_2}$		✓	
K_1 and K_2			✓

TABLE 5 SOURCES OF UNCERTAINTY IN A TRANSFER INSTRUMENT MEASUREMENT.

A detailed theoretical analysis of the uncertainties arising from imperfect tuning of a reflectometer and mismatch at the measurement plane is given in reference [19] and an analysis of the uncertainties arising from the remaining items in Table 5 is given in reference [20]. To avoid excessive duplication the following section will briefly describe the origin and typical magnitude of the uncertainties in Table 5 plus the uncertainty in using the transfer instrument to measure the reflection coefficient of a termination at the measurement plane.

8.1 Uncertainty Arising From Imperfect Tuning and a Mismatched Termination

8.1.1 Imperfect tuning of T1

T1 must be adjusted until the output of D1 is directly proportional to forward going power ie independent of impedance changes to the right of C1. When tuning T1, impedance changes are produced by sliding a short circuit termination on C1; T1 is then adjusted for, typically ± 0.01% variation in the output of D1.

During calibration and use the reflection coefficient of devices at the measurement plane will change from unity to zero. To a very close approximation this change appears at the output of C1 (a 10 dB coupler) as a change from 0.1 to zero. The error in power measurement at D1, arising from imperfect setting of T1, will never be greater than

$$(0.01)\ \frac{0.1}{2} \quad = \quad 0.0005\%$$

during any stage of calibration or use.

8.1.2 Imperfect tuning of T2 and T3

Figure 9 illustrates the second directional coupler of the transfer instrument. T2 is set, with a sliding load at the measurement plane to achieve an isolation of 60 dB between the main arm and side arm of C2. T3 is set, with a sliding short circuit at the measurement plane to reduce the VSWR looking into port 2 (Γ_2) to less than 1.001.

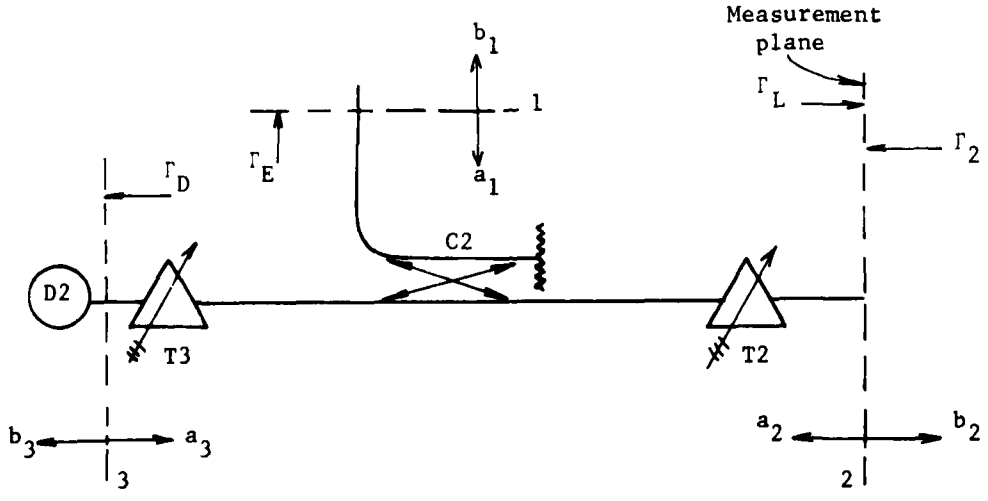

Figure 9. Electric fields (a,b) and reflection coefficients (Γ) at C2

Representing the cascaded scattering matrices of C2, T2 and T3 by S_{11}, S_{12} .....S_{32}, S_{33} and the electric field amplitude at D2 by $|b_3|$, the power absorbed by D2 will be proportional to $|b_3|^2$ and is given by [19]:-

$$|b_3|^2 = \frac{|E|^2 \, |(S_{21}S_{32} - S_{31}S_{22})\Gamma_L + S_{31}|^2}{|1-\Gamma_2\Gamma_L|^2 \, |(1-S_{11}\Gamma_E)(1-S_{33}\Gamma_D) - S_{31}^2 \, \Gamma_E\Gamma_D|^2} \qquad (20)$$

where $E = a_1 - b_1\Gamma_E$.

If T2 and T3 could be set for infinite isolation at C2 and unity VSWR respectively then $S_{31} = \Gamma_2 = 0$ and (20) reduces to:-

$$|b_3|^2 = \left| \frac{E \, S_{21}S_{32} \, \Gamma_L}{(1-S_{11}\Gamma_E)(1-S_{33}\Gamma_D)} \right|^2 \qquad (21)$$

The power at D2 is directly proportional to $|\Gamma_L|^2$ under these conditions.

With a knowledge of the magnitude of the coupler scattering parameters the extreme values of uncertainty in power measurement at D2, arising from imperfect setting of T2 and T3, are given by:-

$$\left[\frac{P}{Q} - 1\right] \qquad (22)$$

where

$$P = \frac{(|S_{21}S_{32}| \pm |S_{31}S_{22}|)|\Gamma_L| \pm |S_{31}|)^2}{(1 \mp |\Gamma_2\Gamma_L|)^2\{(1 \mp |S_{11}\Gamma_E|)(1 \mp |S_{33}\Gamma_D|) \mp |S_{31}^2\Gamma_E\Gamma_D|\}^2} \qquad (23)$$

and

$$Q = \frac{|S_{21}S_{32}\Gamma_L|^2}{\{(1 \mp |S_{11}\Gamma_E|)(1 \mp |S_{33}\Gamma_D|)\}^2} \qquad (24)$$

For a 10 dB directional coupler, tuned to 60 dB isolation, an input VSWR of 1.001 and terminated at the measurement plane in a short circuit, the uncertainty in power measurement is ± 0.77%* (rectangular limits). This is also the uncertainty in determining the ratio K_1/K_2.

---

* Numerical values: $|S_{21}| = 0.316$, $|S_{32}| = 0.950$, $|S_{31}| = 0.001$, $|S_{11}| = |S_{22}| = |S_{33}| = 0.01$, $|\Gamma_E| = 0.04$, $|\Gamma_D| = 0.1$, $|\Gamma_L| = 1$ and $|\Gamma_2| = 0.0005$.

When the transfer instrument is being calibrated the VSWR of the standard bolometer mount will be < 1.02. Substituting $|\Gamma_L| = 0.01$ in (22) to (24) yields an uncertainty in power measurement at D2 (typically 0.9 μW) of ± 78%. Using (16) the effect of ± 78% uncertainty in $(P_3)_{std}$ results in an uncertainty in K_1 of ± 0.009% (rectangular limits).

If the device of unknown efficiency is another bolometer of VSWR <1.02 then, using (18), the effect of ± 78% uncertainty in P_3 results in an uncertainty of ± 0.008% in the unknown value of efficiency. For a device of VSWR equal to 1.2 this uncertainty in efficiency increases to ± 0.07% (rectangular limits).

8.2 Uncertainty Arising From Non-unity Short Circuit Reflection Coefficient

The short circuit used in calibration of the transfer instrument is always an offset short circuit, selected to have its shorting plane one quarter of a guide wavelength away from the measurement plane. This removes the region of high current density from the discontinuity at the flange and minimises field distortion. The finite conductivity of both the shorting plate and the quarter wavelength of waveguide reduce the reflection coefficient at the measurement plane below unity.

A WG16 offset short circuit at 10 GHz yields a reflection coefficient of 0.9996 and a WG22 offset short circuit yields a reflection coefficient of 0.9993 [20]. Equation (14) assumed a perfect short circuit connected to the measurement plane. If an offset short circuit is used whose reflection coefficient is 0.07% less than unity, the best estimate of $\frac{K_1}{K_2}$ will be the measured value plus 0.14%. The corresponding correction at 10 GHz in WG16 is + 0.08%.

8.3 The Effect of Uncertainty in the Efficiency of the Bolometer Standard

The uncertainty in the effective efficiency of the bolometer standard used to calibrate the transfer instrument has been derived in section 6.6 as ± 0.1% (95% CL).* It is apparent from (16) that ± 0.1% uncertainty in power measurement at port 2 of the transfer instrument results in ± 0.1% uncertainty in K_1.

---

* The mount efficiency is determined in a microcalorimeter immersed in a water bath at, typically 26°C. When used for calibrating the transfer instrument the mount will be at ambient temperature, typically 20°C. From the change in conductivity of the copper mount over 6°C temperature change the corresponding efficiency change for a WG18 mount will be 0.003% and 0.007% for a WG22 mount.

8.4 Uncertainty Arising From Noise and Drift in the Power Meters

Limits are imposed on the accuracy of power measurement at D1 and D2 by noise associated with the power meter bridge voltages and thermal drift in the temperature controlled thermistor heads. During calibration in terms of a power standard, and a subsequent measurement, the noise and drift in the standard power meter and device under test will contribute to the random uncertainty in K_1 and η_u respectively. Observation of the noise and drift associated with individual voltages enabled limits to be assigned to these voltages. The overall effect of noise and drift on $\frac{K_1}{K_2}$, K_1 and η_u was determined by evaluating each quantity 200 times whilst randomly varying each voltage within its predetermined limits. The resulting uncertainties in $\frac{K_1}{K_2}$, K_1 and η_u, expressed as 95% confidence limits, are ± 0.002%, ± 0.006% and ± 0.007% respectively; assuming the device under test to be another bolometer mount.

8.5 Uncertainty Arising From Voltage Measurement

The uncertainty in measurement of thermistor and bolometer power meter bridge voltages, using a 6½ digit dvm, was derived from the voltmeter specification and calibration. Using a similar random number generation programme to that used in 8.4 the uncertainties in $\frac{K_1}{K_2}$, K_1 and η_u were derived as ± 0.001%, ± 0.002% and ± 0.002% (95% CL) respectively.

8.6 Effect of Variation in Source Power Level

During a voltage scan with microwave power on, the variation in power from the levelled source is always less than ± 0.02%.

8.7 Overall Uncertainty

The overall uncertainty and correction associated with the measured value of $\frac{K_1}{K_2}$ can be found by combining, in the appropriate manner [8], the components of uncertainty outlined in 8.1 to 8.6. This uncertainty, summarised in Table 6, is then included in the uncertainty budget of K_1. Although the correction to $\frac{K_1}{K_2}$ in Table 6 has been taken as the highest likely to be encountered (+ 0.14% at Q-band) this has no significant effect on K_1. K_2 is calculated from K_1 and the ratio $\frac{K_1}{K_2}$. The device under test, of efficiency η_u, has been assumed in Table 6 to be a bolometer of reflection coefficient 0.01 giving an overall uncertainty of ± 0.14% (95% CL). For a device with a reflection coefficient of 0.1 the increased uncertainty arising from mismatch yields an overall uncertainty of ± 0.2% (95% CL).

Source of Uncertainty	Affecting			
	$\frac{K_1}{K_2}$	K_1	K_2	η_u
Imperfect tuning of T1	± 0.0005 R	± 0.0005 R	*	± 0.0005 R
Imperfect tuning of T2, T3 and mismatch	± 0.77 R	± 0.009 R	*	± 0.008 R
vrc of short circuit	+ 0.14	*	*	*
Standard mount efficiency	*	± 0.1 G	*	*
Noise & drift in power meters	± 0.002 G	± 0.006 G	*	± 0.007 G
Voltage measurement	± 0.001 G	± 0.002 G	*	± 0.002 G
Variation in source power	± 0. 02 G	± 0.02 G	*	± 0.02 G
$\frac{K_1}{K_2}$	*	< 0.0001	- 0.14 ± 0.79	*
K_1	*	*	± 0.12	± 0.12
K_2	*	*	*	< 0.0001
Total correction and overall uncertainty	+ 0.14±0.79	± 0.12	- 0.14 ± 0.80	± 0.14

Note: a) all figures are a percentage

b) 'R' denotes a rectangular distribution, 'G' a Gaussian

c) Corrections are applied to the measured value to yield the best estimate

d) Overall uncertainty is for 95% confidence.

TABLE 6 COMPONENTS OF UNCERTAINTY IN A TRANSFER INSTRUMENT MEASUREMENT

8.8 Uncertainty in Measuring Reflection Coefficient

The most significant uncertainty in using a transfer instrument for reflection coefficient measurements arises from the uncertainties in power measurement at D2 as a consequence of imperfect adjustment of T2 and T3. In practice the reflection coefficient of a device at the measurement plane would be calculated using (19), but this makes no allowance for imperfect tuning. If the output from D1 (fig 8), remains constant while the short circuit and device under test are connected in turn to the measurement plane then (19) simplifies and the right hand side can be expressed as the ratio of two terms derived from (20). Let $|b_{3sc}|^2$ be proportional to the power at D2 with a good short circuit at the measurement plane and $|b_{3u}|^2$ proportional to the power at D2 when the device under test is connected. The reflection coefficient will then be given by:-

$$\left\{\frac{(P_3)_u}{(P_3)_{sc}}\right\}^{\frac{1}{2}} = \left|\frac{b_{3u}}{b_{3sc}}\right| = \left|\left(\frac{1-\Gamma_2}{1-\Gamma_2\Gamma_u}\right)\left(\frac{\Gamma_u + K}{1+K}\right)\right| \qquad (25)$$

where

$$K = \frac{S_{31}}{\begin{vmatrix} S_{21} & S_{31} \\ S_{22} & S_{32} \end{vmatrix}} \qquad (26)$$

NB: When $S_{31} = \Gamma_2 = 0$ the right hand side of (25) reduces to $|\Gamma_u|$

Figure 10 illustrates the limits of uncertainty in a reflection coefficient measurement using (19) with an imperfectly tuned 10 dB coupler.

9 NATIONAL AND INTERNATIONAL POWER COMPARISONS

Having designed, produced and evaluated a standard the most significant phase of its development still remains; namely its authentication. Confidence in the stability of a waveguide power standard can be established by regular, local comparison with similar standards, for example, using a transfer instrument. However, confidence in the absolute validity of the standard can only be gained by comparison with independently developed standards and preferably standards based on fundamentally different principles. The following sections outline recent comparisons, to which some RSRE standards have been subjected.

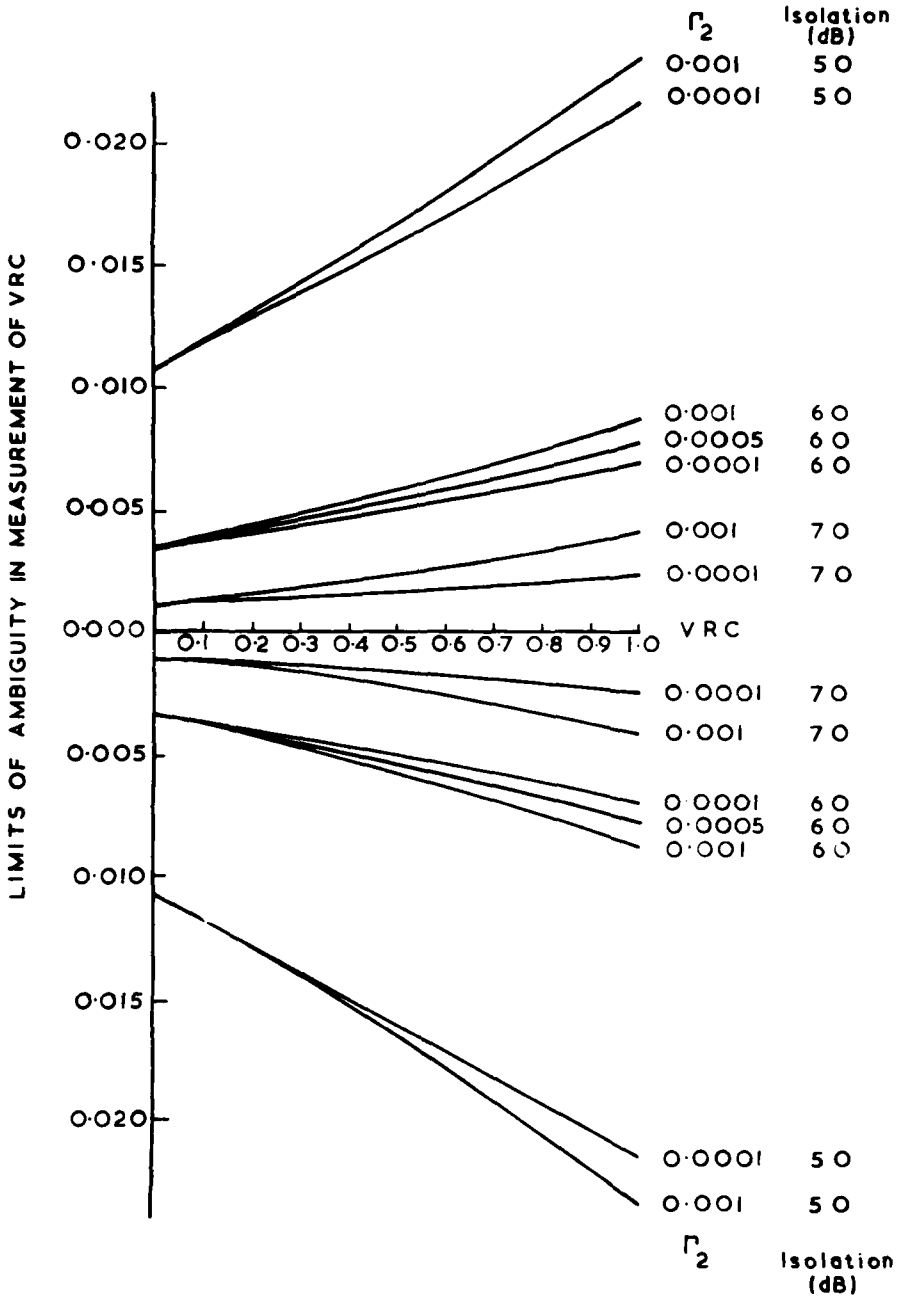

Fig 10 Uncertainty in reflection coefficient measurement arising from imperfect tuning of T2 and T3.

9.1 WG16-WG18 Comparison

To check consistency between mounts calibrated in the WG16 and WG18 microcalorimeters a comparison was performed at 12.4 GHz. Four WG18 bolometer mounts whose efficiency was determined in the WG18 microcalorimeter, were measured, in turn, through three WG16 to WG18 tapers on a calibrated WG16 transfer instrument, ie twelve combinations of mount and taper were used. The taper efficiency when terminated in each WG18 mount was determined using a modification of a technique devised for waveguide to coaxial line adaptors [18]. (The modification involved using the transfer instrument to measure the dissipative attenuation of pairs of tapers connected back-to-back [21]). The efficiency of each WG18 mount was derived in terms of the efficiency of the WG16 mount used to calibrate the transfer instrument and the taper efficiency. Twelve differences in the values of WG18 mount efficiency were obtained during a ten month period and the mean of these differences (WG18 microcalorimeter value - WG16 transfer instrument value) was - 0.04%; the estimated uncertainty in the comparison was ± 0.32% (95% CL).

9.2 Comparison with Coaxial Line Power Standard

The United Kingdom National Standard for power in 14 mm coaxial line consists of a dual load dry calorimeter fitted with a GR 900 connector [22]. It has been developed at the National Physical Laboratory (NPL) and is calibrated at discrete frequencies up to 8.2 GHz. In March 1977 the RSRE waveguide power standards at 8.2 GHz were compared with two of the NPL calorimeters and a 14 mm coaxial line travelling standard calibrated with respect to one of the calorimeters. A WG16 transfer instrument, calibrated in terms of an 8.2 GHz bolometer standard was used to measure the efficiency of the coaxial line calorimeters through a WG16 to GR900 adaptor. Three adaptors were used successively and the efficiency of each was determined, for each coaxial power meter, using the technique described in reference [18]. Full results of this comparison are reported elsewhere [23] but, in summary, twelve combinations of the three power meters with three adaptors (some combinations being repeated) yielded an average difference in power measurement (NPL power - RSRE power) of + 0.05%. Combined NPL and RSRE uncertainties were, typically ± 0.35% (95% CL).

9.3 Comparison with a Flow Calorimeter

Commencing in 1969 with some of the WG16 frequencies listed in section 1, traceability to national waveguide power standards has been provided for the Services Electronic Standards Centre at EQD Aquila. Staff at EQD have developed

a range of dual waveguide flow calorimeters in waveguide sizes from WG10 to WG22 [24]. These enable microwave power measurements, at levels of up to 20W, to be made in terms of dc standards. A traceability exercise involves the calibration of an EQD broadband transfer instrument in terms of the flow calorimeter and use of the transfer instrument to measure the RSRE bolometer standards. By January 1980 sufficient RSRE bolometers had been produced and evaluated to provide traceability at all the frequencies listed in section 1. An indication of the agreement obtained between the bolometers and flow calorimeter over recent years can be obtained from fig 11. For the most recent comparisons (1979 and 1980) the combined estimated uncertainty was ± 0.31% (95% CL).

9.4 International Power Comparison in WG22

In May 1975 RSRE participated in an international comparison of power in WG22 at 34.5 GHz and 35 GHz. Other laboratories participating were NRC (Canada) - the pilot laboratory, NBS (USA) and ETL (Japan). NRC circulated three thermistor mounts as travelling standards. The comparison was completed in 1978 and the results are fully reported in reference [25]. Table 7 shows how the values at individual laboratories compared with the mean of all laboratories (ie the best estimate of 'true' mount efficiency).

Lab	(Individual lab - mean of all labs) %	
	34.5 GHz	35.0 GHz
NRC	+ 0.29	+ 0.26
NBS	- 0.15	- 0.13
RSRE	+ 0.06	+ 0.11
ETL	- 0.20	- 0.24

TABLE 7 DIFFERENCE OF INDIVIDUAL LABORATORIES FROM THE MEAN VALUE OF MOUNT EFFICIENCY (average for three mounts).

At the end of the comparison the thermistor travelling standards (on loan from NRC) were remeasured at 35 GHz at RSRE, both in the WG22 micro-calorimeter and with respect to a calibrated WG22 bolometer mount using the WG22 transfer instrument. Appropriate corrections were applied to the micro-calorimeter results obtained for the bolometer and thermistor mounts to

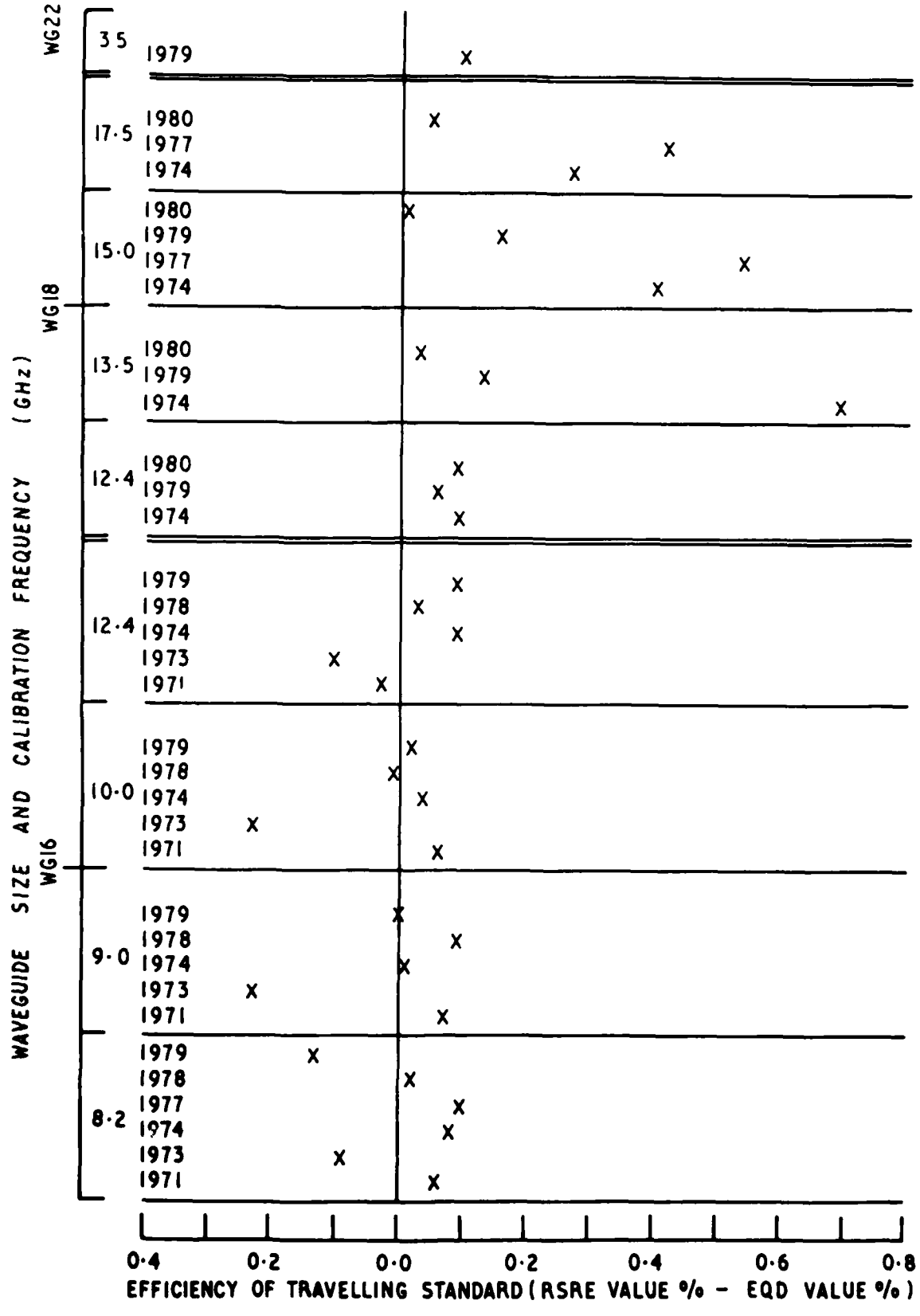

Fig 11 Calibration history for EQD traceability

compensate for input waveguide heating, thermopile offset and microwave leakage. (The variation in thermopile sensitivity between dc and dc plus microwave heating was estimated to be negligible). The resulting values of efficiency of each thermistor mount differed by 0.21%, 0.05% and 0.05%, (water bath value - transfer instrument value). In the context of section 6.5 this result indicates that any rf-dc substitution error in the RSRE bolometer elements, even at 35 GHz, is within the uncertainty in the efficiency determination.

9.5 International Power Comparison in WG18

Measurements in this 15 GHz comparison started in December 1978 with two calibrated RSRE bolometer mounts, of the design in fig 2, being sent to PTB (Germany), the pilot laboratory. They were returned to RSRE in June 1979 accompanied by two PTB bolometer travelling standards and two commercial thermistor mounts. The RSRE and PTB bolometer mounts were calibrated in the WG18 microcalorimeter and the thermistor mounts using the WG18 transfer instrument. The RSRE bolometers had remained stable since their earlier calibration at RSRE. In December 1979 all six mounts were sent to NRC (Canada). Remaining laboratories in the comparison are NBS (USA), LCIE (France) and IEN (Italy).

9.6 International Power Comparison in WG16

To complete the record of RSRE's involvement in international comparisons the results of a 1970 comparison at 9 GHz involving RSRE, NBS (USA) and RIND (Sweden) are summarised in Table 8. The results of measurements on two travelling standards are fully described in reference [1].

Lab	Efficiency of the two travelling standards (%)	
RSRE	99.19	99.18
NBS	99.16	99.17
RIND	99.10	98.98

TABLE 8 SUMMARY OF WG16 COMPARISON

10 PRESENT AND FUTURE PROJECTS

The latest design of X- and J-band bolometer mount appears to satisfy all the criteria of stability, low leakage, high efficiency and low VSWR associated with a single frequency tuned mount. Development and evaluation of Q-band mounts with similar properties and using commercial bolometer elements is well advanced. To increase options on Q-band mount design some effort is being made to produce bolometer elements within RSRE.

The problem associated with quantifying the effect of input waveguide heating (section 6.4) has been avoided in a WG18 microcalorimeter nearing completion. Existing microcalorimeters have two lengths of thermally isolating waveguide and one length of uniform waveguide between the outer calorimeter jacket and the measurement flange (fig 3). The new design has one piece of electroformed waveguide from the measurement flange, through the inner jacket to the outer jacket. Thermal isolation is provided over two sections of the waveguide by reducing the outer dimensions to give a wall thickness of 0.08 mm (0.003"). Electrically the waveguide presents a uniform attenuation constant for 90 mm preceding the flange. From fig 7 it appears that this form of construction should significantly reduce the uncertainty in relating input waveguide heating, measured in the presence of a short circuit, to input waveguide heating during a calibration.

The new microcalorimeter will also incorporate welded thermopiles rigidly mounted on an insulating anulus. The thermopile amplifier will be in good thermal contact with the outer jacket to reduce the effects of dissipation on the thermopile offset voltage.

11 CONCLUSIONS

The latest RSRE design of bolometer mount at X- and J-band has proved to be stable, of high efficiency and low leakage. Six such mounts have been used reliably as National and international travelling standards. Evaluation of the systematic uncertainties described in 6.2 to 6.4 permits 95% confidence limits of ± 0.1% to be assigned to the value of mount efficiency obtained from a microcalorimeter calibration. (± 0.1% was the objective stated in the conclusion of RSRE report 772 [1]). Comparison of RSRE standard bolometer mounts with other National and international power standards has provided increased confidence in the validity of the mount calibration and uncertainty analysis.

Computer control of the calibration process has increased the number of calibrations possible in a 14 day period from 4 to 7 since full use can be made of night-time and week-end working.

Minimising random uncertainty by ensuring good mechanical and temperature stability of the transfer instrument and an analysis of systematic uncertainties, has resulted in automated measurements of efficiency of a matched bolometer mount having an overall uncertainty of ± 0.14% (95% CL).

These developments have resulted in a group of bolometer mounts at X-and J-band and apparatus to calibrate and intercompare them in a manner similar to that used for standard cells in maintaining a dc voltage standard.

12 ACKNOWLEDGEMENTS

The author acknowledges the sound basis provided in the development of waveguide power standards up to 1975 by the late Mr I A Bagnall, Mr J Roberts and Mr S Clark of RSRE. In the past few years the assistance of Mr D R Gordon and Mr L D Hill of RSRE has proved invaluable in bringing the development of waveguide power standards to the state described in this report. For their comments and helpful suggestions on the first draft of this report the author is indebted to Mr C R Ditchfield, Mr E J Griffin, Dr L C Oldfield and Mr F L Warner of RSRE.

13 REFERENCES

1 Bagnall, I A: "The UK standard of microwave power measurement in WG16 and international intercomparisons", RRE Technical Note No 772, Oct 1972.

2 Halford, G J: "Preferred frequencies for calibration and measurement", Paper No 3, Proc Joint IERE-IEE Conf on RF Measurements and Standards, Nov 1967.

3 "Preferred frequencies for electrical measurement", British Calibration Service Publication 4001, Oct 1973.

4 Larsen, N T: "50 microdegree temperature controller", Review of Scientific Instruments, Vol 39, No 1, pp 1-12, Jan 1968.

5 Harvey, M E: "Precision temperature-controlled water bath", Review of Scientific Instruments, Vol 39, No 1, pp 13-18, Jan 1968.

6 Engen, G F: "A refined X-band microwave microcalorimeter", Journal of Research of the NBS - C. Eng & Instrum, Vol 63C, No 1, pp 77-82, Sep 1956.

7 Bagnall, I A, J Roberts and S Clark: "The automated system used in the calibration of the UK waveguide power standards", Conf on Precision Electromagnetic Measurements, Conference handbook, pp 185-187, July 1974.

8 "The expression of uncertainty in electrical measurement", British Calibration Service Publication 3003, April, 1977.

9 Bayer, H: "Microcalorimeter precision measuring equipment for determining the effective efficiency of bolometer measuring heads in the frequency range 8.2 to 12.4 GHz", PTB Mitteilungen 80, pp 261-269, 1970 (In German). (DRIC Translation 4952, Aug 1977 in English).

10 Sucher, M and H J Carlin: "Accuracy of bolometric power measurements", Proc IRE, Vol 40, pp 1042-1048, Sep 1952.

11 Jarvis, S and J W Adams: "Calculation of substitution error in barretters", Journal of Research of the NBS-C, Eng & Instrum, Vol 72C, No 2, pp 127-137, June 1968.

12 Adams, J W and S Jarvis: "Current distribution in barretters and its application to microwave power measurements", IEEE Trans on MTT, Vol MTT-17, No 10, pp 778-785, Oct 1969.

13 Adams, J W and R F Desch: "Experimental confirmation of barretter substitution error", IEEE Trans on MTT, Vol MTT-16, No 3, pp 201-202, Mar 1968.

14 Engen, G F: "A bolometer mount efficiency measurement technique", Journal of Research of the NBS-C, Eng & Instrum, Vol 65C, No 2, pp 113-124, June 1961.

15 Sakurai K and T Maruyama: "A millimetre wave microcalorimeter", IRE Trans on Instrum, Vol IM-11, pp 270-274, Dec 1962.

16 Skilton P J: "A technique for determination of loss, reflection and repeatability in waveguide flanged couplings", IEEE Trans on Instrum & Meas, Vol IM-23, No 4, pp 390-394, Dec 1974.

17 Engen, G F: "A transfer instrument for the intercomparison of microwave power meters", IRE Trans on Instrum, Vol I-9, No 2, pp 202-208, Sep 1960.

18 Skilton, P J: "A technique for measuring the efficiency of waveguide-to-coaxial-line adaptors", IEEE Trans on Instrum & Meas, Vol IM-27, No 3, pp 231-234, Sep 1978.

19 Skilton, P J: "Reflectometry and slotted lines", IEE Vacation school on RF Electrical Measurements, University of Lancaster, pp 11/1-11/44, Jul 1979.

20 Skilton, P J: "Transfer instrument manual", unpublished MOD(PE) Report.

21 Skilton, P J: "A reflectometer and power ratio technique for the measurement of low values of waveguide attenuation", IEEE Trans on Instrum & Meas, Vol IM-25, No 4, pp 307-311, Dec 1976.

22 Fantom, A E: "Improved coaxial calorimetric rf power meter for use as a primary standard", Proc IEE, Vol 126, No 9, pp 849-854, Sep 1979.

23 Skilton, P J and A E Fantom: "A comparison of the United Kingdom National standards of microwave power in waveguide and coaxial lines", IEEE Trans on Instrum & Meas, Vol IM-27, No 3, pp 297-298, Sep 1978.

24 Abbott, N P, C J Reeves and G R Orford: "A new waveguide flow calorimeter for levels of 1-20 W", IEEE Trans on Instrum & Meas, IM-23, No 4, pp 414-420, Dec 1974.

25 Clark, R F, E J Griffin, T Inoue, M P Weidman: "An international intercomparison of power standards in WR-28 waveguide", to be published.

APPENDIX A

DISSIPATION IN A UNIFORM WAVEGUIDE TERMINATED IN (i) A SHORT CIRCUIT, (ii) A MISMATCHED BOLOMETER MOUNT.

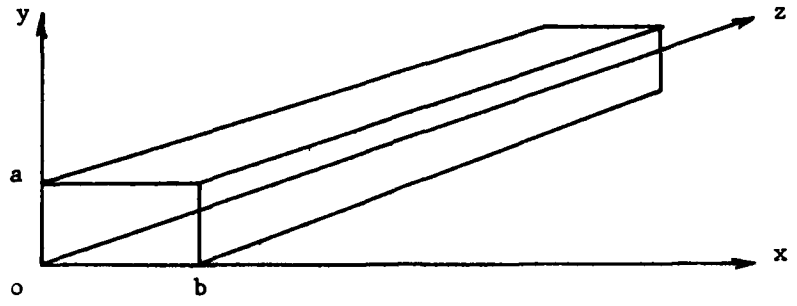

Starting from the solution to the wave equation and imposing boundary conditions the current density at the waveguide walls can be derived as a function of the reflection coefficient (Γ_L) terminating the waveguide. Since power dissipated per unit area of the waveguide walls is the product of the surface resistivity and the square of the current density the ratio of the square of the current densities on changing Γ_L will yield the ratio of waveguide heating effects.

For waveguide in the co-ordinate system shown above, with an air dielectric and propagating in the H_{01} mode

$$E_x = E_z = 0 \quad \text{and} \quad H_y = 0 \tag{A1}$$

The solution of the wave equation for the electric field, E_y, is:-

$$E_y = A \sin \frac{\pi x}{b} \sin (wt - \beta z) \tag{A2}$$

where A is a constant, line losses are assumed to be negligible and $\beta = \frac{2\pi}{\lambda g}$.

Equating components in the directions of the unit vectors $\underline{i}$, $\underline{j}$ and $\underline{k}$ (x, y and z respectively) of

$$\text{Curl } \underline{E} = -\dot{\underline{B}} \tag{A3}$$

(Faraday's law of electromagnetic induction)

with the conditions in (A1) gives:-

$$\frac{\partial E_y}{\partial z} = \mu_o \frac{\partial H_x}{\partial t} \tag{A4}$$

and

$$\frac{\partial E_y}{\partial x} = -\mu_o \frac{\partial H_z}{\partial t} \tag{A5}$$

from which

$$H_x = -\frac{A\beta}{\omega\mu_o} \sin\frac{\pi x}{b} \sin(\omega t - \beta z) \tag{A6}$$

and

$$H_z = \frac{A\pi}{\omega\mu_o b} \cos\frac{\pi x}{b} \cos(\omega t - \beta z) \tag{A7}$$

Equations (A2), (A6) and (A7) completely describe a 'forward' going wave (ie increasing z) in a loss free waveguide.

Considering the specific case of a length of loss free waveguide terminated at $z = 0$ with a reflection coefficient $\Gamma_L = |\Gamma_L|e^{j\theta}$, the real parts of the

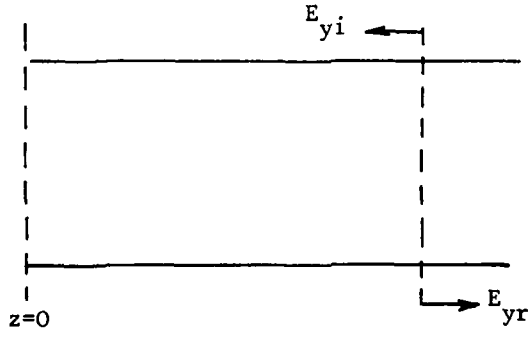

incident and reflected electric fields (E_{yi} and E_{yr}) are given from (A2) as:-

$$E_{yi} = A \sin\frac{\pi x}{b} \sin(\omega t + \beta z) \tag{A8}$$

and

$$E_{yr} = A|\Gamma_L| \sin\frac{\pi x}{b} \sin(\omega t - \beta z + \theta) \tag{A9}$$

Magnetic field components are given by solving (A4) for H_{xi} and H_{xr} and (A5) for H_{zi} and H_{zr}, giving :-

$$H_{xi} = \frac{A\beta}{\omega\mu_o} \sin\frac{\pi x}{b} \sin\psi \tag{A10}$$

$$H_{xr} = -\frac{A\beta\,|\Gamma_L|}{\omega\mu_o} \sin\frac{\pi x}{b} \sin\rho \tag{A11}$$

$$H_{zi} = \frac{A\pi}{\omega\mu_o b} \cos\frac{\pi x}{b} \cos\psi \tag{A12}$$

$$H_{zr} = \frac{A\pi\,|\Gamma_L|}{\omega\mu_o b} \cos\frac{\pi x}{b} \cos\rho \tag{A13}$$

where $\psi = (\omega t + \beta z)$ and $\rho = (\omega t - \beta z + \theta)$ (A14)

Over an element of waveguide surface area dS, the integral of the square of the total magnetic field ($\int |H|^2\, dS$), which is proportional to the square of the current density, can be found from equations (A10) to (A13). At any point in the waveguide the magnetic field is given by:-

$$|H|^2 = |H_{xi} + H_{xr}|^2 + |H_{zi} + H_{zr}|^2 \tag{A15}$$

The dissipation in all four sides of the waveguide can be found by integrating $|H|^2$ over the surface and over a length of waveguide from $z = \ell_1$ to $z = \ell_2$. In a period τ, the dissipation will be proportional to the following integral :-

$$\int_o^{\tau}\int_{\ell_1}^{\ell_2} \left\{ \left[\int_o^b |H|^2\, dx \right]_{y=0} + \left[\int_o^a |H|^2\, dy \right]_{x=0} \right\} dz\,dt \tag{A16}$$

Since the evaluation of such integrals is tedious, only the principal results are shown below. Substitution from (A10) to (A13) in (A15) gives :-

$$|H|^2 = \left[\frac{A}{\omega\mu_o}\right]^2 \left[P\ \beta^2 \sin^2\left(\frac{\pi x}{b}\right) + Q\left(\frac{\pi}{b}\right)^2 \cos^2\left(\frac{\pi x}{b}\right)\right] \tag{A17}$$

where $P = \sin^2\psi - 2|\Gamma_L| \sin\psi \sin\rho + |\Gamma_L|^2 \sin^2\rho$ (A18)

and $Q = \cos^2\psi + 2|\Gamma_L| \cos\psi \cos\rho + |\Gamma_L|^2 \cos^2\rho$ (A19)

Integrating over the height and width of the waveguide gives :-

$$\left[\int_o^b |H|^2\, dx\right]_{y=0} + \left[\int_o^a |H|^2 dy\right]_{x=0} = \left[\frac{A}{\omega\mu_o}\right]^2 \left[\frac{Pb\,\beta^2}{2} + Q\left(\frac{\pi}{b}\right)^2 \left(\frac{2a+b}{2}\right)\right] \tag{A20}$$

Using the substitutions in (A14), (A18) and (A19) equation (A20) can be integrated with respect to z between the limits of $z = \ell_1$ and $z = \ell_2$. Finally integrating with respect to t over a period τ results in a considerable simplification since terms such as

$$\int_o^\tau \cos(2\omega t + k)dt = \frac{\sin\omega\tau\ \cos(\omega\tau+k)}{\omega} \tag{A21}$$

can be ignored when compared with other terms. The complete evaluation of (A16) results in a term proportional to the power dissipated and equal to:-

$$\left[\frac{A}{\omega\mu_o}\right]^2 \frac{\tau}{2} \left\{(1+|\Gamma_L|^2)(\ell_2-\ell_1)(R+b\beta)\frac{\beta}{2} + |\Gamma_L|(R-b\beta)\cos(\beta\{\ell_2+\ell_1\}-\theta)\sin\beta(\ell_2-\ell_1)\right\} \tag{A22}$$

where

$$R = \left(\frac{\pi}{b}\right)^2 \frac{(2a+b)}{\beta} \tag{A23}$$

For the specific case of a waveguide terminated in a short circuit (A22) can be simiplified by letting $|\Gamma_L| = 1$ and $\theta = \pi$. The ratio of dissipation in the waveguide between a short circuit termination and a termination of

reflection coefficient Γ_L is given by:-

$$2\left[\frac{(\ell_2-\ell_1)(R+b\beta)\beta-(R-b)\cos\beta\,(\ell_2+\ell_1)\sin\beta\,(\ell_2-\ell_1)}{(1+|\Gamma_L|^2)(\ell_2-\ell_1)(R+b\beta)\beta+2|\Gamma_L|(R-b\beta)\cos\{\beta(\ell_2+\ell_1)-\theta\}\sin\beta(\ell_2-\ell_1)}\right] \quad (A24)$$

for a well matched mount, if $\ell_1 = 0$ then as ℓ_2 increases the ratio tends to 2; see fig 7.

END

DATE
FILMED
10-80

DTIC